Life Sciences 239 (2019) 117013

Contents lists available at ScienceDirect

Life Sciences

journal homepage: www.elsevier.com/locate/lifescie

Low density lipoprotein receptor (LDLR)-targeted lipid nanoparticles for the delivery of sorafenib and Dihydroartemisinin in liver cancers

Zhengfeng Wang*, Xinxin Duan, Yinghao Lv, Yongfu Zhao

Department of Hepatobiliary Surgery, The First Affiliated Hospital of Zhengzhou University, Zhengzhou, 450052, China

ARTICLE INFO

Keywords:
Orafenib
Dihydroartemisinin
Liver cancer
Low density lipoprotein (LDL)
Lipid nanoparticles

ABSTRACT

Aims: Liver cancer is one of the leading causes of cancer mortality worldwide. Inspired by the biological structure and function of low-density lipoprotein (LDL), in this study, an ApopB-100 based targeted lipid nanoparticles was synthesized to improve the therapeutic efficacy in liver cancer treatment.
Main methods: The biological composition of ApopB is similar to LDL which can effectively increase the targeting efficiency of nanoparticles in LDL receptor (LDLR)-overexpressed liver tumors.
Keyfindings: We have demonstrated that the co-administration of sorafenib (SRF) and Dihydroartemisinin (DHA) could exhibit synergistic anticancer effect in HepG2 liver cancer cells. DHA produced excessive cellular reactive oxygen species (ROS) and induced greater apoptosis of cancer cells. LDL-based SRF/DHA-loaded lipid nanoparticles (LD-SDN) showed remarkable decrease in the cell viability compared to that of either of single drug treated cancer cells. Combination of SRF + DHA resulted in predominant SubG1 proportion of cells. LD-SDN exhibited the highest SubG1 (%) of cells compared to that of any of the individual drugs. Most importantly, robust antitumor response and delayed tumor growth was observed for LD-SDN treated xenograft tumor model. Ki67 proliferation index of LD-SDN (22.1 ± 5.6%) is significantly lesser compared to that of either control (86.2 ± 6.9%) or SRF (75.4 ± 4.89%) or DHA (69.4 ± 6.9%).
Significances: These data provide strong evidence that LDL-mimetic lipid nanoformulations could be utilized as a biocompatible and tumor targeted platform for the delivery of multiple anticancer drugs in cancer treatment.

1. Introduction

GLOBOCAN 2018, an International Agency for Research on Cancer (IARC) showed 18.1 million new cases of cancer with approximately 9.5 million cancer-related deaths in 2018 worldwide. Among these, hepatocellular carcinoma (HCC) or liver cancer constitutes 8.5% of mortality rate [1]. The patients with HCC are expected to increase to 1 million cases worldwide in the future. Patients with liver cancer are most often in the middle or late stage of diagnosis where it is difficult to treat patient with either chemotherapy or surgery or any other localized treatment [2]. Chemotherapy is the popular treatment option used in the clinics other than the surgical procedure [3]. Among all, sorafenib (SRF), a multikinase inhibitor is an FDA approved drug indicated in the treatment of patients with advanced liver cancer [4]. The mechanism of action of SRF involves the downregulation of Ras oncogene and thereby inhibits the vascular endothelial growth factor (VEGF) and platelet-derived growth (PDGF) receptors and inhibits the overall tumor cell proliferation [5]. However, one of the critical obstacles in the use of SRF is the poor physicochemical properties (low aqueous solubility and low oral bioavailability) that reduce the therapeutic efficacy in cancer [6]. Free SRF leads to wide systemic distribution in normal organs and tissues, leading to adverse effects including heart attack, hormone disturbances and myelosuppression. Importantly, higher doses of SRF lead to drug resistance phenomenon in cancer tissues [7,8]. These suggests the inability of single agent therapy in cancer treatment necessitating a need for a second agent that can enhance the therapeutic efficacy of SRF while reduce the associated side effects.

Dihydroartemisinin (DHA) is one of the derivative of artemisinin and shown to exhibit anticancer activity in cancer cells [9]. DHA has been reported to generate reactive oxygen species (ROS) owing to the intramolecular endoperoxide bridge and results in oxidative damage, cell cycle arrest and angiogenesis to the cancer cells [10]. Higher ROS production leads to increased expression of heme oxygenase-1 (HO-1) that will further inhibit the cytodine deaminase (CDA) and induce the cancer cell apoptosis [11]. DHA could be combined with anticancer drugs such as SRF to enhance the anticancer efficacy as well as to minimize the associated adverse effects [12]. In this study, we have explored a combination of SRF + DHA in the treatment of liver cancers.

* Corresponding author.
E-mail address: wangzfchina@163.com (Z. Wang).

https://doi.org/10.1016/j.lfs.2019.117013
Received 26 July 2019; Received in revised form 15 October 2019; Accepted 23 October 2019
Available online 31 October 2019
0024-3205/

However, adverse effects of combinational regimen such as myelosuppression or cardiotoxicity could impact the safety of patients.

Towards the search of new nanomaterials for increased performance of nanocarrier system, the diverse lipids have enabled the engineering and versatility of carrier system [13]. In this regard, lipid nanoparticles such as solid lipid nanoparticles (SLN) has been demonstrated to overcome the limitations of polymeric nanoparticles or micelles and used for cancer targeting applications [14]. The SLN exhibits many advantageous features such as improving the aqueous solubility, improved drug stability, higher drug loading, biocompatibility, biodegradability and ease of scale up [15,16]. It has been reported that many cancer cells (HCC, breast and prostate cancer) upregulate the expression of low-density lipoprotein receptors (LDLR) [17]. Low density lipoprotein (LDL), a major cholesterol transporter has been reported to possess great affinity towards the LDLR. The lipid nanoparticles could be reconstituted with commercially available materials to mimic the biological properties of endogenous LDL [18,19]. Apolipoprotein B-100 (ApoB) can be specially recognized by the LDLR that are overexpressed in the liver cancer cells [20]. Generally, LDL have a core structure consisting of cholesterol esters and fatty acids with a lamella-like shell consisting of either phospholipids or ApoB. The lipid nanoparticles based on LDL has been demonstrated to carry the small molecules and nucleic acids [21]. This strategy could effectively enhance the cycle time and targeting efficiency of nanoparticles.

Herein, we report the combinational anticancer effect of SRF + DHA to enhance the therapeutic efficacy in liver cancer treatment. The SRF + DHA were loaded in lipid nanoparticle surface modified with LDL (ApoB) to improve the cancer targeting applications. We hypothesized that DHA could induce the ROS generation that could inhibit the CDA expression and exhibit cell apoptosis and its combination with SRF is expected to produce synergistic effect. The targeting efficiency of lipid nanoparticle was monitored by confocal laser scanning microscopy (CLSM) and flow cytometer. The ROS generation and cell cycle arrest was evaluated by flow cytometer. Finally, in vivo antitumor efficacy analysis was performed in HepG2 cells-bearing xenograft nude mice and immunohistochemical (IHC) studies were performed on tissue sections.

2. Materials and methods

2.1. Materials

Cholesteryl oleate, glyceryl trioleate (triolein), Cholesteryl, L-α-dioleoyl phosphatidylethanolamine (DOPE) were purchased from Avanti polar lipids, China. Tetrazolium bromide (MTT), Sorafenib and DHA were purchased from Sigma-Aldrich, China. Dialysis bag (MWCO 3500 Da) was purchased from YU WANG, China. ApoB-100 was also purchased from Sigma-Aldrich, China. All other organic solvents were purchased and used without further modifications.

2.2. Preparation of SRF/DHA-loaded LDL-based lipid nanoparticles

The lipid nanoparticle was formulated by solvent-emulsification protocol. The oil phase composed of cholesteryl oleate (30 mg) and triolein (6 mg) as a core-structure lipids were dissolved in 1 ml of chloroform/methanol (2:1) mixture. To this organic mixture, DOPE (20 mg) and cholesterol (4 mg) was added as surface-structure lipids. The organic solvent was shaken well to dissolve all the constituents and then SRF (5 mg) and DHA (5 mg) in 1 ml of organic mixture was added and stirred well. Now, 10 ml of distilled water containing 1% of polyvinyl alcohol (PVA) was added to the lipid solution and vortexed for 5 min. The suspension was sonicated using Branson Sonifier® 450 (20 kHz, duty cycle = 40, output control = 3.5) for 5 min. The emulsion was moved to a rotary evaporator and chloroform was taken out under low pressure at 55 °C. The nanoparticle containing dispersion was collected and centrifuged if necessary to concentrate the drug-loaded nanoparticles. The nanoparticle was incubated with ApoB (LDL) at a weight fraction of 10:1 for 12 h under mild shaking at 37 °C. The nanoparticle was centrifuged and re-dispersed in distilled water and stored at 4 °C. The loading efficiency of dual drugs (SRF and DHA) was evaluated by HPLC method. The Agilent 1100 series apparatus equipped with a diode array UV detector was used for the analysis. An Agilent Eclipse XDB-C18 column (150 × 4.6 mm, 3.5 μm) was to separate the drugs. A mixture of acetonitrile (ACN) and distilled water (DW) containing 0.1% trifluoroacetic acid (TFA) was used in a ratio of 70:30 (v/v) for SRF and 65:35 (v/v) for DHA was used.

2.3. Characterization of synthesized drug-loaded lipid nanoparticles

The hydrodynamic diameters and zeta potential of LD-SDN was evaluated by Zetasizer nano-series Nano-ZS (Malvern, UK). Samples are diluted in the order of 1–10 parts in distilled water and measured at 25 °C in triplicate manner. The particle morphology of LD-SDN was evaluated by transmission electron microscopy (TEM) using Jeol JEM-2000EX, Tokyo, Japan. The particles were counterstained with 4% phosphotungistic acid (PTA) and placed in a carbon-coated copper grid and air dried and the particles were evaluated under TEM at 100 kV. The in vitro drug release was evaluated dialysis method. To conduct release experiment, 1 mg equivalent of SRF and DHA containing freeze dried nanoparticles were dispersed in 1 ml of buffer and stored in dialysis membrane clipped from both ends. The dialysis membrane was placed in a tube containing PBS (pH 7.4) and ABS (pH 5.0) buffer. ABS (pH 5.0) was prepared by dissolving 5.77 g of sodium acetate (82 g/mol) and 1.77 g of acetic acid (60.05 g/mol) in 800 ml of water and pH is adjusted to pH 5.0 using 1 M HCl and finally made up to 1000 ml. PBS (pH 7.4) was prepared by dissolving 20.21 g of Disodium hydrogen phosphate heptahydrate (268.07 g/mol) and 3.39 g of Sodium Dihydrogen Phosphate Monohydrate (137.99 g/mol) in 800 ml of water and pH adjusted to pH 7.4 (using HCl or NaOH) and volume made up to 1000 ml. The tube was placed in an orbital shaker maintained at 100 rpm speed at 37 °C. At selected time, 1 ml of sample was withdrawn and replaced with same amount of buffer and the study was continued until 60 h incubation time. The amount of drug release at specific time was determined by HPLC method.

2.4. Cellular uptake and targeting ability of LDL-based lipid nanoparticles

The HepG2 cells were cultured in RPMI 1640 media containing 10% FBS and 1% antibiotic mixture. The cells were incubated and grown in automated incubator maintained at 5% CO_2. For the experiment, HepG2 cells were seeded in 6-well plated at a density of 2×10^5 cells per well and incubated for 24 h. Rhodamine B was used as a fluorescent tracker and loaded in the nanoparticles. The cells were exposed with free Rhodamine B and separately treated with SDN and LD-SDN and incubated for 3 h. The cells were washed thrice with PBS and fixed with 4%paraformaldehyde. The cells were then stained with DAPI as a nuclear staining and then washed again and observed under fluorescence microscope (Nikon A1, Japan). For quantitative analysis, cellular uptake was analyzed by flow cytometer. HepG2 cells were seeded in 6-well plated at a density of 2×10^5 cells per well and incubated for 24 h. The cells were exposed with SDN and LD-SDN and incubated for 3 h. The cells were then washed thrice with ice-cold PBS and extracted and re-suspended in 1 ml of PBS buffer for flow cytometer analysis (BD FACSCalibur, USA).

2.5. Western blot analysis

HepG2 cells were seeded in 6-well plated at a density of 3×10^5 cells per well and incubated for 24 h. The cells were treated with respective formulations and incubated for 24 h. The cells were washed, harvested and treated with lysis buffer for 30 min. The cell suspension was centrifuged at 12000 rpm for 10 min and supernatant

was collected and evaluated for protein concentration using BCA protein assay protocol. The samples were equally loaded in SDS-PAGE gel and separated at 80 V for 2 h. The proteins were transferred to nitrocellulose membrane for 1 h and then blocked with 5% skim in TBST buffer. The membrane was incubated with primary antibodies of BAX, Bcl-2 and GAPDH (1:1000 dilutions) at 4 °C overnight. Next day, membrane was treated with HRP-conjugated secondary antibodies (1:3000 dilutions) for 1 h. The protein expression was evaluated by ECL kit.

2.6. Cell viability assay

The cell viability assay was performed by MTT assay protocol. In brief, 1×10^4 amount of HepG2 cells were seeded in 96-culture plate and allowed overnight to attach. The cells were treated with free SRF, DHA, SDN and LD-SDN in a concentration ranging from 0.01 μg/ml to 20 μg/ml. Separately, combination of SRF + DHA in a weight ratio of 1:1 was used to determine the synergistic index. The cells were then incubated for 24 h under ambient conditions. After 24 h, cells were washed and treated with 10 μl of MTT dye (5 mg/ml) was added to each well and incubated for 4 h. The formazan crystals were formed and solubilized with 100 μL of stop solution (20% (w/v) SDS in 50% (v/v) DMF. The absorbance of formazan crystal was studied at 570 nm using a microplate reader (Berthold Technologies, Germany). The IC50 value was calculated from GraphPad Prism 6.0 software (GraphPad Software, CA, USA). The experiments were performed in quadruplet.

2.7. Cellular ROS analysis

The reactive oxygen species (ROS) production by cancer cells were detected by the oxidation of DCFDA into fluorescent DCF dye. In brief, 2×10^5 amount of HepG2 cells were seeded in 12-culture plate and allowed overnight to attach. The cells were treated with free SRF, DHA, SDN and LD-SDN at a base concentration of 5 μg/ml and incubated for 24 h. After 24 h, cells were trypsinized and washed with PBS two times. The cells were incubated with DCFDA dye (10 μM) for 10 min and then washed two times to remove the excess of dye. The cells were re-suspended in 500 μl of PBS and quantitatively measured for ROS level using flow cytometer (BD FACSCalibur™, BD Bioscience, USA).

2.8. Cell cycle analysis

The cell cycle assay was performed to evaluate the cell cycle progression of cancer cells. In brief, 2×10^5 amount of HepG2 cells were seeded in 12-culture plate and allowed overnight to attach. The cells were treated with free SRF, DHA, SDN and LD-SDN at a base concentration of 5 μg/ml and incubated for 24 h in a humidified CO_2 incubator. After 24 h, cells were trypsinized and washed with PBS two times. The cells were fixed in 70% of ice-cold methanol and washed again with PBS. Followed by, cells were re-suspended in 300 μl of PBS containing 50 μg/ml of RNase and 50 μg/ml of PI at 37 °C in a humidified CO_2 incubator for 15 min. The cells were washed again with PBS twice to remove the excess of PI dye and then re-suspended in 1X PBS and cell cycle progression was quantified by flow cytometer. Untreated cells were used as a negative control.

2.9. In vivo antitumor efficacy

All animal experiments were carried out in accordance to the guidelines framed by Institutional Animal Care and Use Committee of First Affiliated Hospital of Zhengzhou University, Zhengzhou. A 6-week old BALB/c nu/nu nude mouse was procured from the inhouse Animal Facility Center and maintained ambient conditions with free access to food and water throughout the study period. The nude tumor mice model was developed by injecting 150 μl of HepG2 cancer cells (1×10^7) to the right flank of each mice. The experiment was started when the tumor volume reached 100 mm^3. The tumor mice were randomly divided into 5 groups containing 8 mice in each group. The mice were administered with 5 mg/kg of either SRF or DHA via tail vein injection for 3 times with a frequency of once in every 3 days. The combination dose includes 2.5 mg of each drug mixed in a 1:1 ratio in the nanoparticles. The groups include non-treated control, SRF, DHA, SDN and LD-SDN, respectively. The tumor volume was measured using a Vernier caliper and body weight was monitored at every time point. The formula for tumor volume calculation is: Volume (mm^3) = 0.5 × length × $width^2$. The mice were sacrificed, and tumors were extracted, fixed and embedded in paraffin. The tumor section was subjected to immunohistochemical analysis.

2.10. Statistical analysis

All data were presented as means ± standard deviation (SD). Statistical analysis was performed on Software SPSS17.0. Statistical differences were evaluated using the one-way ANOVA and *$P < 0.05$ was considered to be significant.

3. Results and discussion

3.1. Synthesis and characterization of LDL-based SLN formulations

The aim of this study was to improve the therapeutic outcome of liver cancer by encapsulating SRF and DHA in an LDL surface modified solid lipid nanoparticles (Fig. 1). Firstly, dual drugs were loaded in SLN and surface modified with Apolipoprotein B-100 that can specifically recognize the LDLR in the cancer cells. The SLN formulation was prepared with a hydrophobic core containing SRF and DHA with a lamella-like shell consisting of either phospholipids or ApoB. The drug-loaded SLN was physicochemically characterized. The SRF and DHA showed entrapment efficiency (EE) of 94.5 ± 1.62% and 92.1 ± 1.21%, respectively. LD-SDN showed a loading efficiency (LE) of 13.5 ± 0.85% and 12.8 ± 1.12% for SRF and DHA, respectively. Dynamic light scattering (DLS) analysis revealed an average particle size of 115.4 ± 1.25 nm with a narrow polydispersity index (PDI~0.112) for SDN. The particle size of LD-SDN slightly increased to 126.5 ± 1.33 nm with a PDI of 0.135 after the surface modification with LDL (Fig. 2a). The small size of lipid nanoparticle will enhance the prospect of enhanced systemic circulation that will in turn allow the increased accumulation in the tumor tissues via enhanced permeation and retention (EPR) effect. Zeta potential is important physical factor required to maintain the stability of nanoparticles through the electrostatic repulsion between particles. SDN and LD-SDN showed a zeta potential around −23 mV to −25 mV enough to maintain the stability by avoiding the particle aggregation and keeping the long-term stability. TEM image showed a uniform dispersion of spherical shaped particle without any sign of aggregation. The drug-loaded nanoparticles were perfectly spherical shaped with monodispersed range of particles (Fig. 2b).

The in vitro drug release kinetics was performed in order to evaluate the release rate of two drugs in different pH conditions. In the present study, pH 7.4 and pH 5.0 was selected to mimic the physiological an acidic environment in the body conditions (Fig. 2c and d). As shown in Fig. 4, both SRF and DHA released less than 20% within 24 h and overall less than 40% of drug released after 60 h incubation under physiological conditions. This feature of LD-SDN is advantageous as it will avoid the potential side effects of free drug in systemic circulation and avoid the adverse effects to organs. In contrast, drug release of SRF and DHA significantly increased in the acidic conditions from LD-SDN. Approximately 36–38% of drug released within 24 h and 70–80% of drug released after 60 h incubation. The accelerated drug release of SRF and DHA in acidic conditions is beneficial for the cancer treatment. Higher concentration of drug release in the tumor tissue will increase the intracellular concentration and increased therapeutic efficacy. The

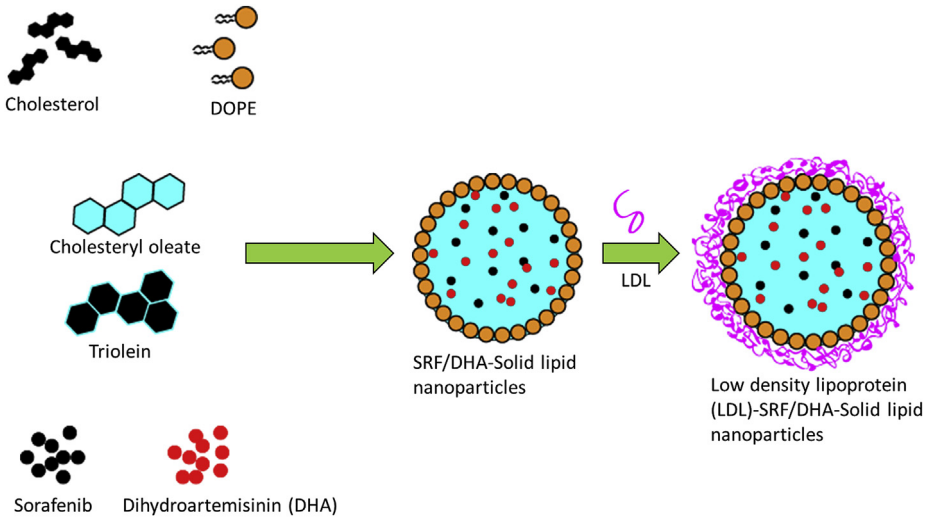

Fig. 1. Schematic illustration of preparation of low density protein (LDL)-based lipid nanoparticles loaded with sorafenib (SRF) and dihydroartemisinin (DHA). The lipid nanoparticles consisting of core lipids and surface structure lipids and ApoB-100 on the particle surface.

release kinetics of LD-SDN is ideal for tumor treatment due to the pH difference in the normal tissues and tumor tissues. Generally, release of drugs from the nanoparticle is one of the key parameters towards the success of cancer drug delivery.

3.2. Targeting efficiency of LD-SDN nanoformulations

It has been reported that LDL based drug delivery carriers could targeting the LDLR which is overexpressed in the various cancer cells including liver cancer cells (HepG2) [22–24]. We anticipated that the presence of LDL as a targeting ligand on the nanoparticle surface could enhance the intracellular level of drugs in the specific tumor cells. To evaluate the targeting efficiency of LDL-based nanoformulations, HepG2 cells were exposed with SDN and LD-SDN formulations. Rhodamine B was used as a fluorescent tracker. These nanoparticles were incubated to the cancer cells and incubated for 3 h. Results showed that SD-LDN could be internalized in the tumor cells more effectively than that of SDN (Fig. 3a). As shown, LD-SDN showed brighter red fluorescence compared to that of SDN indicating the higher cellular uptake in the cancer cells which is in turn attributed to the specific affinity of LDL towards the LDLR which is overexpressed in the HepG2 cancer cells. A quantitative analysis if uptake behavior was carried out using flow cytometer. The flow cytometer histogram of LD-SDN showed a predominant shift in the histogram towards the right side compared to that of SDN indicating a remarkably higher uptake (Fig. 3b). Our results are consistent with the previous findings that LDL modification of nanoparticle could improve the targeting efficiency of carrier towards the liver cancer cells. Results clearly demonstrated that LDL-based nanoformulations were internalized into tumors via LDLR-related endocytosis [25].

3.3. In vitro anticancer effect

The in vitro anticancer effect was first determined by MTT assay. As

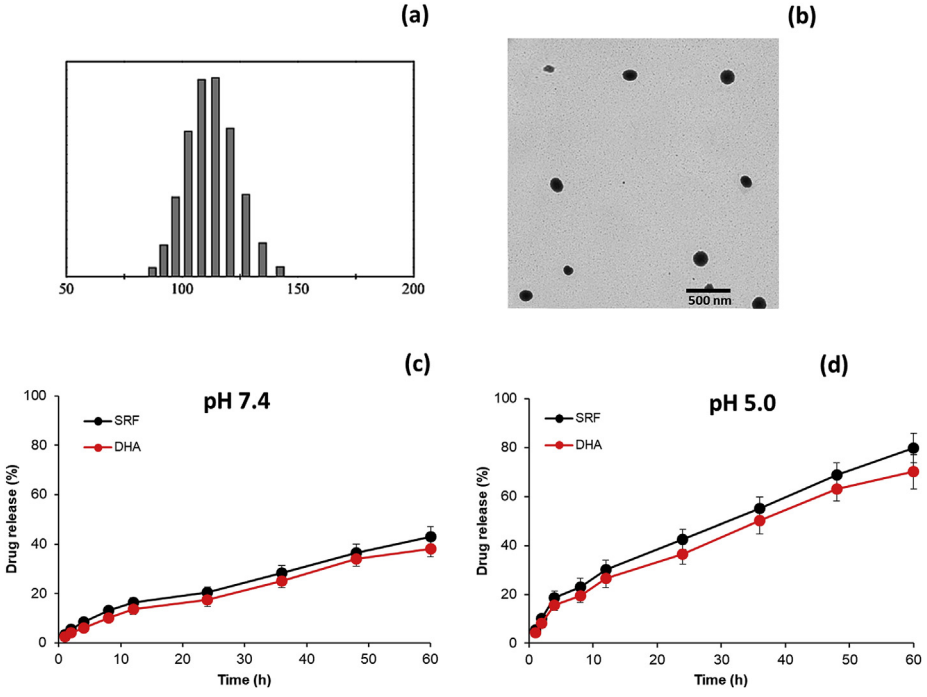

Fig. 2. Physicochemical characterization of LD-SDN. (a) Hydrodynamic diameters and particle size distribution; (b) particle morphology of LD-SDN using transmission electron microscopy (TEM); (c,d) in vitro release patterns of SRF and DHA from LD-SDN in physiological (pH 7.4) and acidic (pH 5.5) conditions. The drug release was quantified by HPLC method.

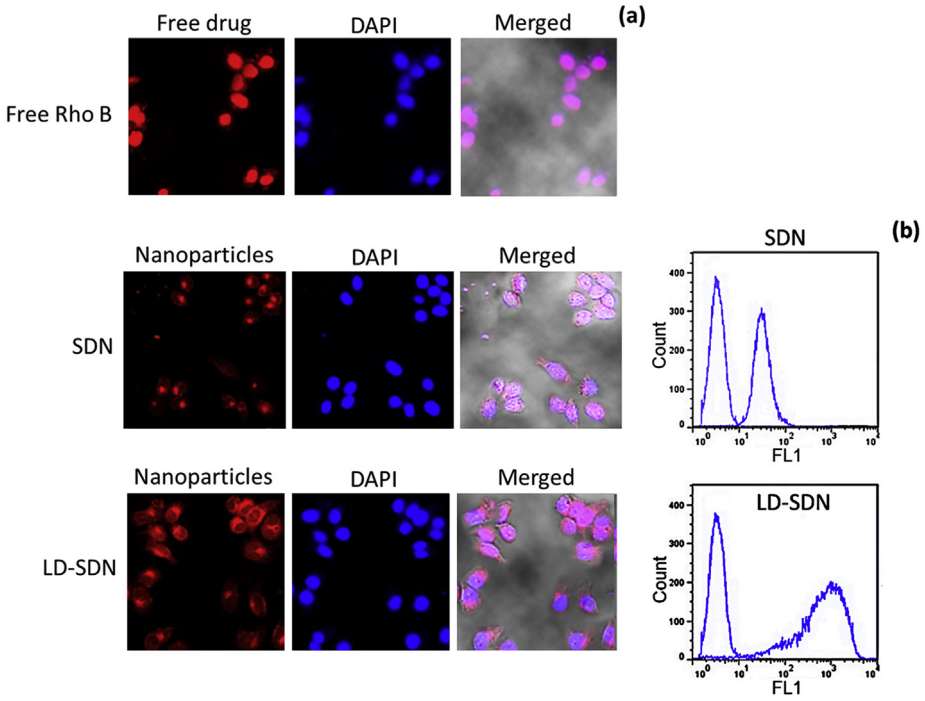

Fig. 3. Targeted delivery of LD-SDN in liver cancer cells. (a,b) Confocal laser scanning microscopy (CLSM) and flow cytometer analysis of cellular uptake of SDN and LD-SDN in HepG2 cancer cells. The uptake of nanoparticles in cancer cell was tracked by the loading of Rhodamine B. 10 μg of blank NP was used for the experiment.

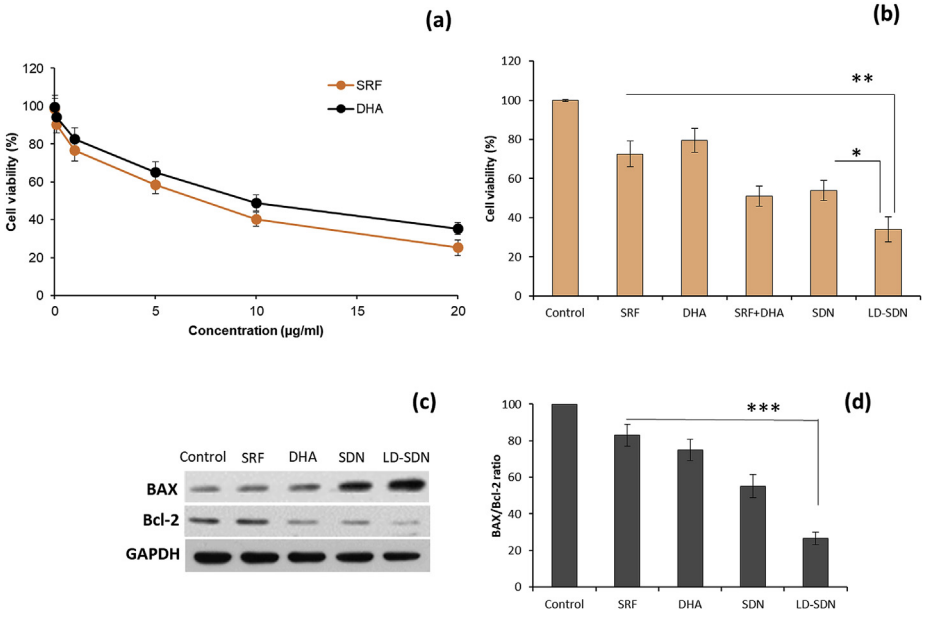

Fig. 4. Cell viability analysis of nanoformulations. (a) Dose-dependent cytotoxic effect of SRF and DHA in HepG2 cancer cells; a maximum of 120 μg of blank NP was employed for the cell viability assay; (b) cell viability analysis of HepG2 cells after treatment with SRF, DHA, SDN and LD-SDN, respectively and a fixed dose of 2.5 μg of respective drug was used; (c,d) Western blot analysis of protein expression after treatment with respective formulations. *$p < 0.05$ is the statistical difference between SDN and LD-SDN and **$p < 0.01$ between LD-SDN and SRF. A fixed dose of 2.5 μg of respective drug was used and 150 μg of blank NP was employed.

shown, both SRF and DHA showed a concentration-dependent reduction in the cell viability of HepG2 cancer cells (Fig. 4a). The IC50 value of SRF and DHA were 4.12 μg/ml and 7.65 μg/ml, respectively. The results showed that SRF was more effective in killing cancer cells compared to that of DHA as a single drug alone. Next, single and combinational regimen of drugs was tested in HepG2 cancer cells. Before that, blank nanoparticles (LDL-conjugated) at different concentrations were tested in HepG2 cancer cells and observed to possess no toxic effect even in highest tested concentration indicating the biocompatible nature of solid lipids (Fig. S1). Later, HepG2 cells were treated with free SRF, free DHA, SDN and LD-SDN and incubated for 24 h. As expected, treatment of either SRF or DHA at 1 μg/ml resulted in moderate decrease in the cell viability (Fig. 4b). In contrast, combination of SRF + DHA as SDN resulted in significant reduction in the cell viability and more importantly, LD-SDN showed remarkable decrease in the cell viability. The cell viability assay with free drug combo has observed insignificant difference between SDN and LD-SDN. It is worth noting that free drug or free drug combo induce notable anticancer effect in the in vitro conditions, however, it will exhibit poor therapeutic outcome in the in vivo conditions owing to the immediate clearance of small molecules from the blood circulation and induce toxicity to the vital organs. On average, 2-fold reduction in cell viability was observed for LD-SDN treated cancer cells compared to that of either of single drug treated cancer cells. The higher cytotoxic effect of SRF + DHA might be attributed to that synergistic chemotherapeutic effect. The combination index (CI) was calculated using the Chou and Talalay's

method. The CI value of LD-SDN at 1:1 wt ratio was 0.35 indicating a strong synergism in the anticancer activity. Cellular uptake experiment confirmed the higher internalization capacity of LD-SDN that might increased the intracellular concentration and higher cell killing effect. Mechanistically, DHA could induce the production of intracellular ROS generation that suppressed the CDA expression. The lower CDA expression combined with the multikinase inhibitory effect of SRF contributed to the synergistic anticancer effect. Western blot analysis further proved the combinational effect [26]. As shown, SDN and LD-SDN significantly decreased the BAX/Bcl-2 ratio compared to that of single drugs (SRF and DHA). Bcl-2 and BAX constitutes the important apoptosis related regulator genes in the Bcl-2 protein family and its level are indicator of apoptosis (Fig. 4c and d). DHA could potentially increase the ROS levels that might increase the apoptosis in the cancer cells [27].

3.4. Combination of SRF + DHA on the generation of ROS analysis

ROS plays an important role in the apoptosis and death of cancer cells. ROS generation is higher in cancer cells compared to that of normal cells and higher oxidative stress could regulate the expression of signaling pathways and cell death. To confirm the potential of DHA to increase the cytotoxicity of SRF by acting on the ROS generation, we have used flow cytometer analysis after staining with DCFH-DA probe (Fig. 5). As shown, combination of SRF + DHA induced the higher ROS generation as shown by the higher shift the DCFA-DA based fluorescence shift (DCF fluorescence intensity in cancer cells). SRF did not have much influence on the ROS generation as shown the flow cytometer data. The DHA in the combination regimen produced excess of ROS in the tumor cells. The Endoperoxide Bridge in DHA structure upon breaking produces the oxygen free radicals and increases the ROS level in the cancer cells [28]. The increase in the ROS level in the current study attributed to the combinational effect of SRF and DHA. The higher levels of ROS could result in irreparable oxidative destruction to lipids and intracellular DNA resulting in cell death [29].

3.5. Induction of apoptosis by SRF + DHA combination

In order to further investigate whether ROS generation and cytotoxicity caused by the combination of SRF + DHA was associated with apoptosis and cell cycle arrest, flow cytometer analysis was carried out. SubG1 phase is considered to be apoptosis phase of cell cycle. The cells were treated with SRF, DHA, SDN and LD-SDN and then quantified by flow cytometer after PI staining. Individual drugs (SRF or DHA) displayed cell cycle arrest at G2/M phase with fewer cells in SubG1 phase compared to that of control (Fig. 6). Combination of SRF + DHA resulted in predominant SubG1 proportion of cells. LD-SDN exhibited the highest SubG1 (%) of cells compared to that of any of the individual drugs. LD-SDN exhibited a 3-fold higher SubG1% of cells and SDN showed 2-fold higher SubG1% of cells compared to SRF or DHA alone. These data clearly substantiated the cell viability and ROS analysis where combination of drugs exhibited higher anticancer effect compared to that of single drugs.

3.6. Antitumor efficacy in HepG2 tumor animal model

Inspired by the remarkable anticancer effect of nanoformulations at in vitro conditions, antitumor efficacy of SRF, DHA, SDN, and LD-SDN was evaluated in HepG2 cancer cell-bearing xenograft tumor model. The mice were administered with the above said formulations 3 times with a frequency of once in 3 days via tail vein injection and tumor volume/body weight was noted periodically. Results showed that free SRF and DHA were effective than control only during the initial time points (time of drug administration) and then rapidly grew insignificant to that of non-treated control group. Recently, Jing et al. demonstrated that combination of Sorafenib (SRF) and Artesunate (ART) (a prodrug of Dihydroartemisinin) exhibits significant tumor volume reduction

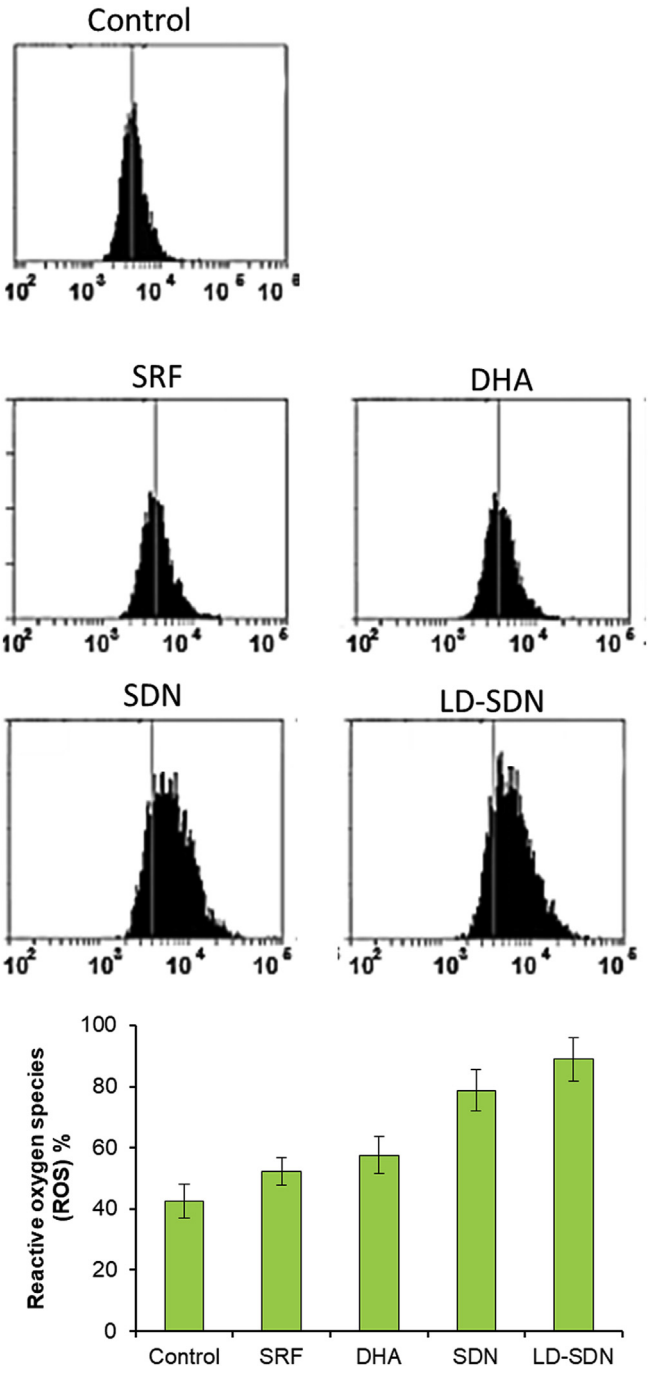

Fig. 5. Reactive oxygen species (ROS) generation of cancer cells after treatment with respective formulations. The cells were treated with DCFH-DA and intracellular ROS levels were assessed by flow cytometry. A fixed dose of 2.5 μg of respective drug was used and 150 μg of blank NP was employed.

compared to that of individual SRF or ART. However, authors employed a dose of 2.5 mg/kg of SRF +100 mg/kg of ART and administered every other day for 4 weeks [30]. Similarly, in another study, Zhang et al., have used a combo of 5 mg/kg of each SRF + doxorubicin (DOX) which almost displayed insignificant effect as that of non-treated control, however, SRF/DOX-loaded NP was significantly more effective compared to that of free drug combo [31]. Similarly, Yang et al., showed that free drug combo (SRF + Cisplatin) showed significantly higher anticancer effect than the individual free drug at 5 mg/kg each (5 times administration), however, significantly less compared to that of SRF/Cisplatin-loaded NP [32]. It is apparent that combo drugs

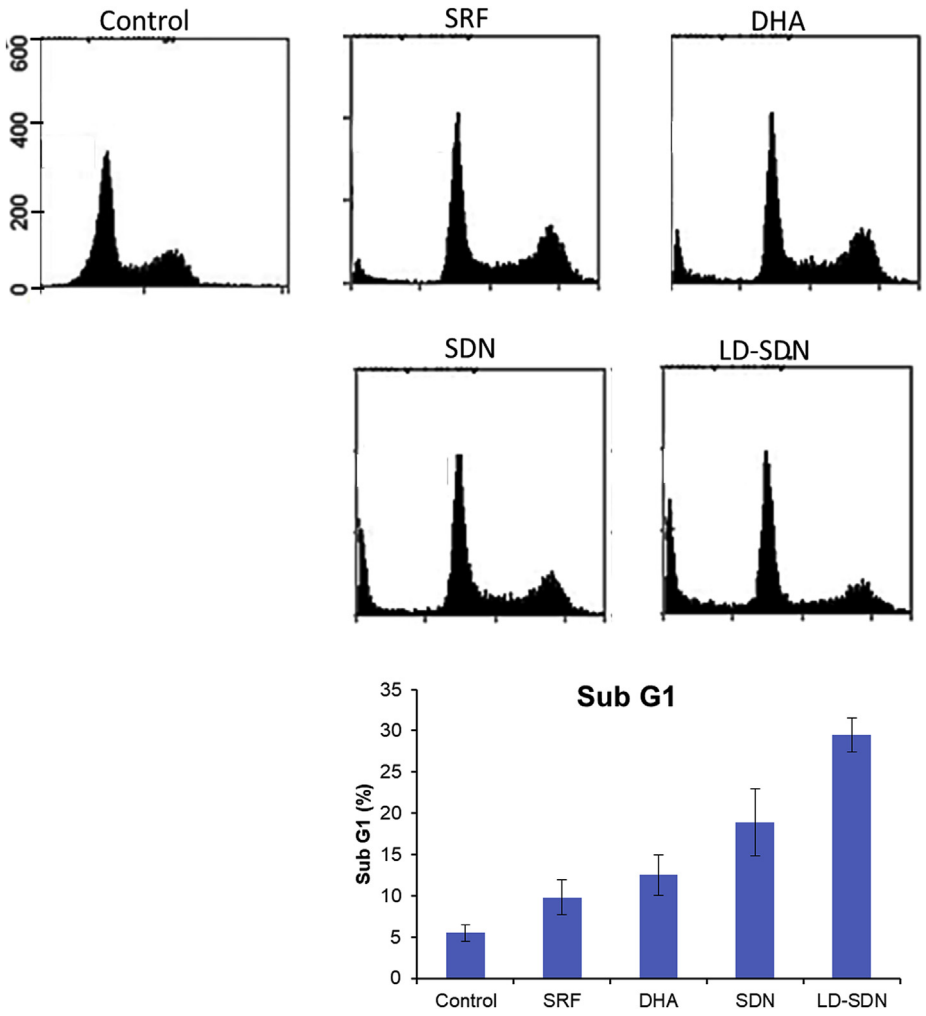

Fig. 6. Cell cycle arrest of cancer cells after treatment with respective formulations. The cell cycle analysis was analyzed using flow cytometer after staining with PI dye. A fixed dose of 2.5 μg of respective drug was used and 150 μg of blank NP was employed.

exhibited better anticancer effect than free single drug treatment, however, in all the cases, it was significantly less compared to that of nanocarrier-based combination drugs, therefore, we have only focused on the dual drug-loaded nanoparticles (targeted and non-targeted). Interestingly, as expected dual drug-loaded lipid nanoparticles (SDN) effectively reduced the tumor burden in HepG2 tumor model compared to that of individual drugs alone (Fig. 7a and b). Throughout all time points, significant difference in tumor volume was observed between SDN and SRF or DHA alone indicating the synergistic anticancer effect of combinational regimen. Most importantly, robust antitumor response and delayed tumor growth was observed for LD-SDN treated animal group. Compared to animals treated with free drugs (individual), LD-SDN treated animals did not show multifold increase in tumor volume even after the last administration of formulations indicating the potent antitumor effect of this group. The final tumor volume of Control, SRF, DHA, SDN, and LD-SDN groups were ~1900 mm^3, ~1700 mm^3, ~1150 mm^3, and ~600 mm^3, respectively. Similar results were observed in the tumor weight calculations. LD-SDN showed a 4-fold decrease in tumor volume than those of control while it is 3-fold decreased compared to that of free drugs. The enhanced antitumor effect of LD-SDN might be attributed to that enhanced tumor homing property of tumors towards these nanoformulations. The modification of lipid nanoparticles with LDL acted as a targeting ligand towards the LDLR which is overexpressed in the liver cancers and contributed to the higher accumulation of nanoparticles in the tumor tissues. The effective encapsulation of two drugs in lipid nanoparticles, minimal release in physiological environment and maximal release of drugs in the acidic tumor environment might be one of the important factors for enhanced antitumor effect of LD-SDN [33–35]. Moreover, body weight was monitored as a typical indicator of the drug toxicity. As shown, SRF shed more than 10% of body weight at day 7 and day 10 compared to that of control. DHA treated group shed more than 5% of body weight at day 7 (Fig. 8a).

Animals from both the group recovered the body weight towards the end of the study. In contrast, drug loaded nanoparticles (SDN and LD-SDN) did not show any sign of body weight loss during any point in the study period indicating the safety index of the drug delivery system. Such system with higher anticancer effect with no body weight loss will be of great important in cancer treatment.

It is worth noting that Guo et al. have demonstrated that particle elasticity may contribute to alter the internalization pathways of nanoparticles [36]. Guo et al. showed that soft NLP-45KPa enters the cell through two independent pathways (fusion and endocytosis) while, the elastic NLGs may enter the cell only through endocytosis, that requires membrane bending, and coated pits; requiring cells to take more time and energy to internalize the same amount of NLG-19MPa as opposed to NLP-45KPa. Whereas, Jiang and Shi et al. have showed a higher tumor uptake of lipid-coated poly(lactic-co-glycolic) acid (PLGA) NPs, and they reported that rigid lipid-coated PLGA NPs like SLN in the present study enter cell more efficiently than soft ones [37,38]. This could be due to that fact that lipid-coated PLGA NPs are significantly more rigid than NLP45 KPa and at such high elasticity; clathrin-

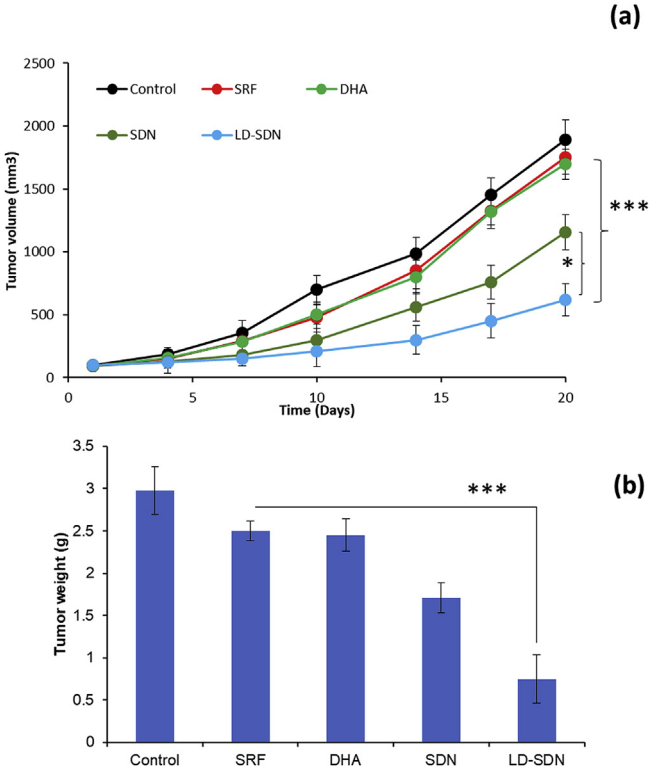

Fig. 7. In vivo antitumor effect of SD-LDN formulations. (a) Tumor growth curves of nude mice-bearing HepG2 tumors were recorded after intravenous administration of SRF, DHA, SDN and LD-SDN formulations via tail vein at a fixed concentration of 5 mg/kg; (b) tumor weight analysis of each group. *p < 0.05 is the statistical difference between SDN and LD-SDN and ***p < 0.001 between LD-SDN and SRF. A maximum of 600 μg of blank NP was employed for each group at each administration.

mediated endocytosis becomes the dominant cell internalization pathway for both rigid and soft lipid-coated PLGA NPs. Based on these facts, it is safe to assume that LD-SDN with possibly high elasticity might internalize predominantly via clathrin-mediated endocytosis and resulted in higher anticancer efficacy.

3.7. Immunohistochemistry

The mice were sacrificed, and tumors were extracted and immunohistochemical analysis (IHC) performed. The tumor cell proliferation was evaluated by Ki67 positive cell populations (Fig. 8b and c). The dark brown stains indicate the Ki67 expression in the tumor tissues. As shown, Ki67 proliferation index of LD-SDN (22.1 ± 5.6%) is significantly lesser compared to that of either control (86.2 ± 6.9%) or SRF (75.4 ± 4.89%) or DHA (69.4 ± 6.9%). These results clearly indicate that administration of LD-SDN resulted in significant damage to the tumor tissues and effectively cut down the growth of tumor cells and delayed the tumor volume.

4. Conclusion

In summary, we have established a unique delivery system to encapsulate the combinational regimen of SRF + DHA to enhance the antitumor efficacy in liver cancers. LDL was effective in exhibiting higher cellular internalization and enhanced tumor homing property in LDLR overexpressed liver cancers. We have demonstrated that DHA could induce the ROS generation and combination of SRF + DHA would exhibit the synergistic anticancer effect in HepG2 cancer cells. In vivo antitumor study displayed a robust antitumor response and delayed tumor growth for LD-SDN in HepG2 tumors with substantially lower Ki67 + cells. Overall, LD-SDN could serve as a specific tumor targeting carrier to enhance the therapeutic efficacy in liver cancers. This biocompatible lipids-derived nanoparticle holds immense potential to treat multiple other tumors.

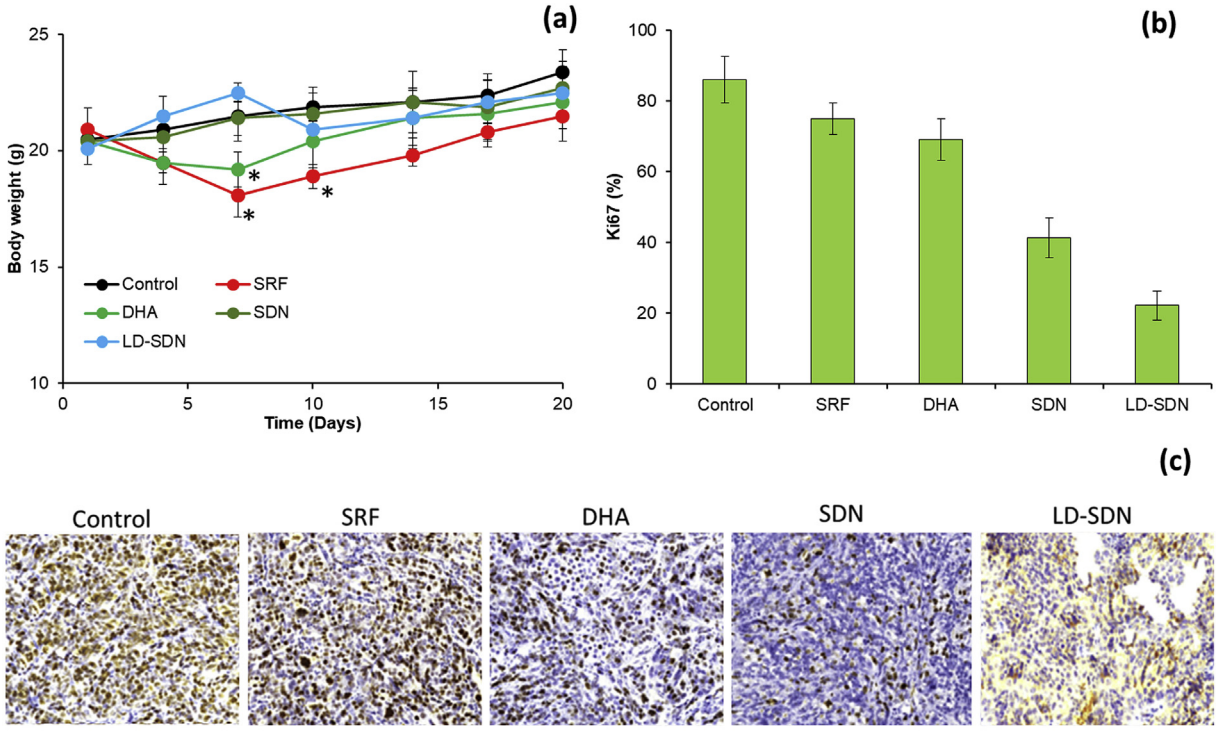

Fig. 8. (a) Body weight analysis of nude mice at specified time point; (b,c) Immunohistochemical assays of Ki67 protein in the tumor section. The Ki67 + is indicated by the dark brown staining of the nuclei. *p < 0.05 is the statistical difference between SDN/LD-. (For interpretation of the references to colour in this figure legend, the reader is referred to the Web version of this article.)

Author's contributions

XD and YL were involved in the preparation and preliminary characterization of lipid nanoparticles. YZ performed biological experiments and along with ZW were involved in the tumor animal study. And ZW designed and wrote the entire manuscript.

Declaration of competing interest

The authors report no declarations of interest.

Acknowledgement

This study was supported by Youth Fund from the First Affiliated Hospital of Zhengzhou University, China.

Appendix A. Supplementary data

Supplementary data to this article can be found online at https://doi.org/10.1016/j.lfs.2019.117013.

References

[1] F. Bray, J. Ferlay, I. Soerjomataram, Global cancer statistics 2018 : GLOBOCAN estimates of incidence and mortality worldwide for 36 cancers in 185 countries, CA can, J. Clin. 68 (2018) 394–424.
[2] H.M. Moukhadder, R. Halawi, M.D. Cappellini, A.T. Taher, Hepatocellular carcinoma as an emerging morbidity in the thalassemia syndromes: a comprehensive review, Cancer 123 (2017) 751–758.
[3] Y. Li, D. Zhu, L. Hou, et al., TRB3 reverses chemotherapy resistance and mediates crosstalk between endoplasmic reticulum stress and AKT signaling pathways in MHCC97H human hepatocellular carcinoma cells, Oncol. Lett. 15 (2018) 1343–1349.
[4] J.M. Llovet, R. Montal, D. Sia, R.S. Finn, Molecular therapies and precision medicine for hepatocellular carcinoma, Nat. Rev. Clin. Oncol. 15 (2018) 599–616.
[5] S. Wilhelm, C. Carter, M. Lynch, T. Lowinger, J. Dumas, R.A. Smith, B. Schwartz, R. Simantov, S. Kelley, Discovery and development of sorafenib: a multikinase inhibitor for treating cancer, Nat. Rev. Drug Discov. 5 (2006) 835.
[6] M. Cervello, G. Pitarresi, A.B. Volpe, B. Porsio, D. Balasus, M.R. Emma, A. Azzolina, R. Puleio, G.R. Loria, S. Puleo, G. Giammona, Nanoparticles of a polyaspartamide-based brush copolymer for modified release of sorafenib: in vitro and in vivo evaluation, J. Control. Release 266 (2017) 47–56.
[7] A.L. Cheng, Y.K. Kang, Z. Chen, C.J. Tsao, S. Qin, et al., Efficacy and safety of sorafenib in patients in the Asia-Pacific region with advanced hepatocellular carcinoma: a phase III randomised, double-blind, placebo-controlled trial, Lancet Oncol. 10 (2009) 25–34.
[8] Z. Zhang, B. Niu, J. Chen, X. He, X. Bao, J. Zhu, H. Yu, Y. Li, The use of lipid coated nanodiamond to improve bioavailability and efficacy of sorafenib in resisting metastasis of gastric cancer, Biomaterials 35 (2014) 4565–4572.
[9] P. Li, S. Yang, M. Dou, Y. Chen, J. Zhang, X. Zhao, Synergic effects of artemisinin and resveratrol in cancer cells, J. Cancer Res. Clin. Oncol. 140 (2014) 2065–2075.
[10] N. Gao, A. Budhraja, S. Cheng, E.H. Liu, C. Huang, J. Chen, Z. Yang, D. Chen, Z. Zhang, X. Shi, Interruption of the MEK/ERK signaling cascade promotes dihydroartemisinin-induced apoptosis in vitro and in vivo, Apoptosis 16 (2011) 511–523.
[11] Z. Huang, X. Huang, D. Jiang, Y. Zhang, B. Huang, G. Luo, Dihydroartemisinin inhibits cell proliferation by induced G1 arrest and apoptosis in human nasopharyngealcarcinoma cells, J. Canc. Res. Therapeut. 12 (2016) 244–247.
[12] Y.Y. Lu, T.S. Chen, X.P. Wang, L. Li, Single-cell analysis of dihydroartemisininduced apoptosis through reactive oxygen species-mediated caspase-8 activation and mitochondrial pathway in ASTC-a-1 cells using fluorescence imaging techniques, J. Biomed. Opt. 15 (2010) 046028.
[13] T. Ramasamy, H.B. Ruttala, B. Gupta, et al., Smart chemistry-based nanosized drug delivery systems for systemic applications: a comprehensive review, J. Control. Release 258 (2017) 226–253.
[14] T.T. Hiep, T. Ramasamy, H.J. Cho, et al., Formulation and optimization of raloxifene-loaded solid lipid nanoparticles to enhance oral bioavailability, J. Nanosci. Nanotechnol. 14 (2014) 4820.
[15] P. Yingchoncharoen, D.S. Kalinowski, D.R. Richardson, Lipid-based drug delivery systems in cancer therapy: what is available and what is yet to come, Pharmacol. Rev. 68 (2016) 701–787.
[16] M.A. Oberli, A.M. Reichmuth, J.R. Dorkin, M.J. Mitchell, O.S. Fenton, A. Jaklenec, D.G. Anderson, R. Langer, D. Blankschtein, Lipid nanoparticle assisted mRNA delivery for potent cancer immunotherapy, Nano Lett. 17 (2017) 1326–1335.
[17] L.A. Pires, R. Hegg, F.R. Freitas, E.R. Tavares, C.P. Almeida, E.C. Baracat, Effect of neoadjuvant chemotherapy on low-density lipoprotein (LDL) receptor and LDL receptor-related protein 1 (LRP-1) receptor in locally advanced breast cancer, Braz. J. Med. Biol. Res. 45 (2012) 557–564.
[18] G. Hu, X. Chun, Y. Wang, Q. He, H. Gao, Peptide mediated active targeting and intelligent particle size reduction-mediated enhanced penetrating of fabricated nanoparticles for triple-negative breast cancer treatment, Oncotarget 6 (2015) 41258–41274.
[19] A. Stranzl, H. Schmidt, R. Winkler, G.M. Kostner, Low-density lipoprotein receptor mRNA in human breast cancer cells: influence by PKC modulators, Breast Canc. Res. Treat. 42 (1997) 195.
[20] A. Kader, P.J. Davis, M. Kara, H. Liu, Drug targeting using low density lipoprotein (LDL): physicochemical factors affecting drug loading into LDL particles, J. Control. Release 55 (1998) 231–243.
[21] J. Herz, M.S. Brown, Calcium cages, acid baths and recycling receptors, Nat. Int. Weekly Jo. Sci. 388 (1997) 629–630.
[22] J. Guillemot, M.C. Asselin, D. Susan-Resiga, R. Essalmani, N.G. Seidah, Deferoxamine stimulates LDLR expression and LDL uptake in HepG2 cells, Mol. Nutr. Food Res. 60 (2016) 600–608.
[23] J.H. Yang, M.A. Bang, C.H. Jang, G.H. Jo, S.K. Jung, S.H. Ki, Alginate oligosaccharide enhances LDL uptake via regulation of LDLR and PCSK9 expression, J. Nutr. Biochem. 26 (2015) 1393–1400.
[24] S. Cao, P. Xu, J. Yan, H. Liu, L. Liu, L. Cheng, F. Qiu, N. Kang, Berberrubine and its analog, hydroxypropyl-berberrubine, regulate LDLR and PCSK9 expression via the ERK signal pathway to exert cholesterol-lowering effects in human hepatoma HepG2 cells, J. Cell. Biochem. (2018), https://doi.org/10.1002/jcb.27102.
[25] J.C. Mazière, C. Mazière, S. Emami, et al., Processing and characterization of the low density lipoprotein receptor in the human colonic carcinoma cell subclone HT29¬18: a potential pathway for delivering therapeutic drugs and genes, Biosci. Rep. 12 (1992) 483–494.
[26] J. Bai, X. Jia, W. Zhen, W. Cheng, X. Jiang, A facile ion-doping strategy to regulate tumor microenvironments for enhanced multimodal tumor theranostics, J. Am. Chem. Soc. 140 (2018) 106-109.
[27] D. Trachootham, J. Alexandre, P. Huang, Targeting cancer cells by ROS-mediated mechanisms: a radical therapeutic approach, Nat. Rev. Drug Discov. 8 (2009) 579-591.
[28] P.A. Berman, P.A. Adams, Artemisinin enhances heme-catalysed oxidation of lipid membranes, Free Radic. Biol. Med. 22 (1997) 1283–1288.
[29] R. Kong, G. Jia, Z.X. Cheng, Y.W. Wang, M. Mu, S.J. Wang, S.H. Pan, Y. Gao, H.C. Jiang, D.L. Dong, B. Sun, Dihydroartemisinin enhances Apo2L/TRAILmediated apoptosis in pancreatic cancer cells via ROS-mediated up-regulation of death receptor 5, PLoS One 7 (2012) e37222.
[30] W. Jing, L. Shuo, X. Yingru, M. Min, Z. Runpeng, X. Jun, H. Dong, Artesunate promotes sensitivity to sorafenib in hepatocellular carcinoma, Biochem. Biophys. Res. Commun. 519 (2019) 41–45.
[31] J. Zhang, J. Hu, H.F. Chan, M. Skibba, G. Liang, M. Chen, iRGD decorated lipid-polymer hybrid nanoparticles for targeted co-delivery of doxorubicin and sorafenib to enhance anti-hepatocellular carcinoma efficacy, Nanomedicine 12 (2016) 1303–1311.
[32] F. Yang, A. Li, H. Liu, H. Zhang, Gastric cancer combination therapy: synthesis of a hyaluronic acid and cisplatin containing lipid prodrug coloaded with sorafenib in a nanoparticulate system to exhibit enhanced anticancer efficacy and reduced toxicity, Drug Des. Dev. Ther. 12 (2018) 3321–3333.
[33] T.C. Chou, Drug combination studies and their synergy quantification using the Chou-Talalay method, Cancer Res. 70 (2010) 440-446.
[34] T. Ramasamy, H.B. Ruttala, N. Chitrapriya, et al., Engineering of cell microenvironment-responsive polypeptide nanovehicle co-encapsulating a synergistic combination of small molecules for effective chemotherapy in solid tumors, Acta Biomater. 48 (2017) 131–143.
[35] T. Ramasamy, H.B. Ruttala, K. Kaliraj, K. Poudel, S.G. Jin, H.G. Choi, S. K Ku, C.S. Yong, J.O. Kim, Polypeptide derivative of metformin with the combined advantage of a gene carrier and anticancer activity, ACS Biomater. Sci. Eng. 10 (2019) 5159–5168.
[36] P. Guo, D. Liu, K. Subramanyam, B. Wang, J. Yang, J. Huang, D.T. Auguste, M.A. Moses, Nanoparticle elasticity directs tumor uptake, Nat. Commun. 9 (2018) 130.
[37] J. Sun, et al., Tunable rigidity of (polymeric core)-(lipid shell) nanoparticles for regulated cellular uptake, Adv. Mater. 27 (2015) 1402–1407.
[38] L. Zhang, et al., Microfluidic synthesis of hybrid nanoparticles with controlled lipid layers: understanding flexibility-regulated cell–nanoparticle interaction, ACS Nano 9 (2015) 9912–9921.